Dept. of Math. University of Oslo
Mechanics and Applied Mathematics No. 3
ISSN 0809–4403 December 2004

Implementation of high resolution tidal current fields in electronic navigational chart systems

B. Gjevik[1], D. Hareide[2], B. K. Lynge[2],
A. Ommundsen[3], J. H. Skailand[4], H. B. Urheim[2]

December 16, 2004

Abstract

A system for displaying tidal currents in an electronic chart display and information system (ECDIS) has been developed and implemented in compliance with the standards of the International Hydrographic Organization (IHO). The tidal current fields can be displayed in real time on the electronic navigational chart and several options and functions for updating and zooming have been designed. The current fields are calculated from a data base with the harmonic constants for the four major tidal constituents. The harmonic constants are obtained from a high resolution numerical model which is validated by comparing with sea level and current measurements. The depth matrix for the central part of the model domain was calculated from data from multi-beam bathymetric surveys. An application example of the implementation is given for Trondheimsleia, a part of the main sailing route along the western coast of Norway.

1 Introduction

Tides are an unique oceanographic phenomena in the sense that the tidal motion can be predicted with a high degree of accuracy long time ahead. The art of tidal prediction is based on the knowledge of the harmonic constants of the tidal oscillations and the astronomical arguments i. e. the position of the Sun and the Moon. The harmonic constants can be determined by harmonic analysis of long records of sea level or current obtained either by field observations or by numerical modeling (Foreman 1978).

Tidal modeling has been the subject of numerous studies with world wide applications and the basic techniques have become well established (Davies 1997a,b and references therein). The increase in computer power has made it possible to model large ocean areas with high spatial grid resolution. This means that today the tidal current can be simulated by numerical models with the necessary resolution to provide

[1]Department of Mathematics, University of Oslo, P.O.Box 1053, Blindern, 0316 Oslo, Norway. Email: bjorng@math.uio.no
[2]The Norwegian Hydrographic Service, Stavanger, Norway
[3]Norwegian Defense Research Establishment, Kjeller, Norway
[4]C-MAP Norway A/S, Egersund, Norway

useful information for navigation and marine operations in narrow coastal waters with complex bottom topography and coastlines.

The introduction of multi-beam sounding systems and the Global Positioning System (GPS) have dramatically improved the ability to acquire accurate high-resolution bathymetric data. This development has made it possible to calculate high quality depth matrices for tidal models and hence improve the performance of the models particularly in shallow water.

The electronic chart system is a relatively new technology that provides significant benefits in terms of navigation safety and improved operational efficiency. Electronic charts used in an electronic chart system is a real-time navigation aid that integrates a variety of information. In the Electronic Chart Display and Information System (ECDIS) it is also possible to include time variable navigational objects representing the dynamic variability of the elements surrounding the ships. These objects are known under the term Marine Information Objects (MIOs). MIOs consists of chart- and navigation-related information that supplement the minimum information required in ECDIS to ensure safety of navigation at sea and conforming the IMO Performance Standard for ECDIS. Oceanographic parameters like tides, currents and waves and meteorological parameters like wind speed, wind direction and movement of weather systems are examples of MIOs.

In this paper we will demonstrate that by utilizing the state of the art technology within the three fields; bathymetric surveying, tidal modeling, and electronic chart systems a new navigation tool can be developed where accurate tidal current fields can be displayed in real time in the electronic navigational charts.

The area chosen for this demonstration is a fjord area, called Trondheimsleia, on the western coast of Norway (fig. 1). The tidal range is about 3 m, with relatively strong tidal current in the narrow channels in and out of the fjords. The tidal current dominates the current variability in the area. Trondheimsleia is a main sailing lane for ship traffic along the Norwegian coast. The area is used for aquaculture, fish farming, and also subject to various industrial development projects. Coastal management and environmental protection are therefore important tasks. All these activities will benefit in different ways from the development of an easily accessible operational system for real time display and predictions of the tidal current in the area.

2 The tidal model

Current fields are simulated by the depth-integrated shallow water equations, formulated in flux form in a Cartesian coordinate system (x, y, z) with the x and y axis in the horizontal plane and the z axis vertical:

$$\frac{\partial U}{\partial t} + \frac{\partial}{\partial x}(\frac{U^2}{H}) + \frac{\partial}{\partial y}(\frac{UV}{H}) - fV = -gH\frac{\partial \eta}{\partial x} - c_D\frac{\sqrt{U^2+V^2}}{H}\frac{U}{H} \tag{1}$$

$$\frac{\partial V}{\partial t} + \frac{\partial}{\partial x}(\frac{UV}{H}) + \frac{\partial}{\partial y}(\frac{V^2}{H}) + fU = -gH\frac{\partial \eta}{\partial y} - c_D\frac{\sqrt{U^2+V^2}}{H}\frac{V}{H} \tag{2}$$

where (U, V) specify the components of volume flux vector per unit length in the horizontal plane, η the vertical displacement of the sea surface from the mean sea level, $H = H_0+\eta$ the total depth, H_0 the mean depth, g acceleration of gravity, f the Coriolis

parameter, c_D the drag coefficient of the quadratic bottom shear stress. In addition the continuity equation reads:

$$\frac{\partial \eta}{\partial t} = -\frac{\partial U}{\partial x} - \frac{\partial V}{\partial y} \tag{3}$$

The depth mean current velocity is defined by

$$\overline{u} = \frac{U}{H}, \quad \overline{v} = \frac{V}{H}$$

For the model domain consider here the direct effect of the tide generating forces is negligible, and the tidal motion is mainly driven by the boundary input i.e. sea surface elevation and volume fluxes. In the present problem these equations span a wide parameter range from weak tidal flows on the deeper part of the shelf to strong tidal currents at the coast. The test area used in this application study is for most parts relatively deep and the non linear advection terms in eqs. (1) and (2) are of minor importance and can therefore be neglected. The equations are discretized on a C-grid, (Mesinger and Arakawa 1976) , with a semi-implicit numerical scheme. This scheme has been widely used for depth-integrated ocean models. A discussion of its dispersion and stability properties is given by Martinsen et al. (1979) and Gjevik (1990).The stability criterion satisfied by the numerical time step, Δt, is:

$$\Delta t \leq \frac{\Delta x}{\sqrt{2gH_{max}}},$$

where Δx is the grid size and H_{max} is the maximum depth in the model domain.

The tidal motion is decomposed in harmonic components. For the sea surface displacement this can be written

$$\eta(x, y, t) = \sum_n h_n \cos(\omega_n t - \chi_n - g_n) \tag{4}$$

where ω_n is the angular velocity, the corresponding period $T_n = 2\pi/\omega_n$, h_n and g_n are the harmonic constants, amplitude and phase respectively. These are functions of x and y; $h_n = h_n(x, y)$ and $g_n = g_n(x, y)$. The harmonic constants can be determined by harmonic analysis of the simulated time series in every grid point of the model(Foreman 1978). The phase function χ_n is the astronomic argument which is determined by the position of the Sun and the Moon, (Schwiderski 1980).

Table 1: List of major harmonic components.

Symbol	*Period (T_n) hours*	Frequency (ω_n) 10^{-4} rad/s	*Description*
M_2	12.42	1.40519	principal lunar, semi-diurnal
S_2	12.00	1.45444	principal solar, semi-diurnal
N_2	12.66	1.37880	elliptical lunar, sem-idiurnal
K_1	23.93	0.72921	declinational luni-solar, diurnal

When the harmonics constants are determined, either from measurements or from modeling, the time series for the sea surface displacement can be calculated from eq. (4). A similar harmonic decomposition can be made for the components of the mean current

$$\overline{u}(x,y,t) = \sum_n \overline{u}_n \cos(\omega_n t - \chi_n - g_n^u) \tag{5}$$

$$\overline{v}(x,y,t) = \sum_n \overline{v}_n \cos(\omega_n t - \chi_n - g_n^v) \tag{6}$$

where $\overline{u}_n$,$\overline{v}_n$ and g_n^u,g_n^v are respectively the harmonic constants for the current components. It can be shown that the current vector for each harmonic component describes an ellipse, which is called the tidal current ellipse. The major and minor half axes of the ellipse denoted A and B, respectively, and the orientation of the major axis (θ) can be calculated from the harmonic constants for the current components (Foreman 1978).

In this paper we limit the study to the three major semi-diurnal components M_2, S_2, and N_2 and the diurnal component K_1, (Table 1). Hence the sums in eqs. (4-6) are truncated to n=4. The long period modulation of the tide over a 18.6 year cycle due to the nodal variation of the Moon is also neglected.

3 Model domain and boundary conditions

The high resolution model domain is a 56.7 km × 78.6 km fjord area in Trondheimsleia on the west coast of Norway (fig. 2). The central fjord channels are relatively deep with maximum depth down to about 600 m. The model is nested into coarser grid regional model domain with grid size Δx = 500 m (fig. 1) which covers a larger area 380 km × 383 km. The boundary conditions for the regional model is obtained by interpolating surface elevation and volume fluxes data from a coarse ocean model (Δx = 25 km) for the Norwegian and Barents Seas (Gjevik et al. 1994). The flow relaxation scheme (*FRS*), (Martinsen and Engedahl 1987), has been used to impose the boundary conditions. The rationale behind this scheme is to soften the transition from an exterior solution (here the interpolated data) to an interior solution (model area) by use of a grid zone where the two solutions dominate at each ends respectively. The width of the zone is taken to be ten grid cells. Two types of boundary forcing (exterior solutions) has been tested; i) only surface elevation specified and ii) both surface and and volume fluxes specified. For the regional model domain harmonic constants for the most important harmonic components M_2, S_2, N_2 and K_1 have been calculated and the model has been validated by comparing with sea level and current observations from a large number of stations (Moe et al. 2003).

A similar approach has been adopted for the the high resolution model for Trondheimsleia where interpolated surface elevation and volume fluxes from the regional model are used as boundary conditions at the open boundaries in the west, north and east (fig. 2) to drive the model.

4 Generation of a high resolution depth matrix

The process of generating an accurate depth matrix with grid resolution of $\Delta x = 50$ m for the model domain is done in three steps; bathymetric survey, data processing and griding.

All hydrographic surveys were carried out by the Norwegian Hydrographic Service (NHS). Approximately 35% of the model domain is covered by modern multibeam bathymetric surveys. This includes the central parts of the fjord and the main sailing route in Trondheimsleia from west of current measurement station 2 to east of station 11 (fig. 2). The northern part of the model domain is based on single beam bathymetric surveys while minor areas outside the central part of the domain is based on interpolated data from the depth matrix with 500 m grid resolution (Moe et al. 2003).

The multi-beam bathymetric data was collected in 1999 using a Simrad EM 1002 multi-beam echo sounder. This echo sounder operates from approximately 20 m and down to a depth of 1000 m. The EM 1002 has a accuracy surpassing the International Hydrographic Organization standard S-44 Order 1 and 2 (IHO 1998). Multi-beam echo sounders acquire soundings across a swath of seabed using a collection of acoustic beams. In order for the multi-beam system to calculate accurate x, y and z positions, precise measurements of speed of sound and ship and transducer movements are required. The depth accuracy using Simrad EM 1002 is decreasing from 0.26 m at a depth of 10 m to 0.28 m at a depth of 150 m for beams at nadir (vertical, center beam). For beams 45° off-nadir the depth accuracy is decreasing from 0.24 m at a depth of 10 m to 0.46 m at a depth of 150 m (Øvstedal 2002). Together with the multi-beam sounding system NHS is using Differential GPS (Global Positioning System) for horizontal positioning. The accuracy of the horizontal positions using DGPS is better than 1 m (determined statistically at the 95 % confidence level) and with a standard deviation of 0.5 m (Øvstedal 2002).

The single beam data was surveyed in 1971-1979 and the data was collected as discrete point data along survey vessel track lines with Atlas echo sounders and Simrad EQ echo sounders. The horizontal resolution of single beam acoustic data is defined by the sampling interval along the track lines and the spacing between the track lines. In shallow water the distance between the track lines is much denser than in deep water. An obvious limitation of these conventional single beam surveys is that no quantitative depth information is obtained between survey lines. Submerged rocks and anomalous features detected during the surveys were examined in greater detail. The depth accuracy, determined statistically at the 95% confidence level, for the single beam measurements during the 1970-ies is estimated to 0.6 m at a depth of 10 m depth decreasing to 2 m at a depth of 100 m (Øvstedal 2002). In 1964 NHS started to use Decca Hi-Fix as positioning system for the survey vessels. The Motorola Mini Ranger positioning system was introduced in 1977. The standard deviation of the horizontal positions is estimated to 5 m using the Motorola Mini Ranger (Øvstedal 2002). For the Decca Hi-Fix system there is no good estimates available.

The multi-beam data surveyed in 1999 was processed using the Neptune software developed by Kongberg Simrad (1999) and the NHS. Using the statistical data cleaning module BinStat in Neptune, spikes and other erroneous measurements from the echo sounder are easily removed from the data set, and this is all done under strict quality control. By using Varde (developed by the NHS) to produce triangulated irregular network (TIN) and Cfloor (developed by Cfloor AS) for digital terrain modeling the

xyz-data from Neptune is quality controlled before the data is approved and stored in Hybas, the hydrographic database at the NHS (Aksland 2003).

For some areas the data was only available as fair sheets. The fair sheets were based on single beam data surveyed in 1971-1979 and several weeks were required to transfer the fair sheets by manual digitizing, to a digital format. The resulting digital data was visualized, correlated and analyzed to determine if the data was collected according to international specifications. The resulting and approved data was stored as xyz-data in Hybas.

The Cfloor software is used through the process of making a depth matrix based on bathymetry data from the hydrographic database Hybas. The coastline part of the model originates from a standardized mapping database owned and maintained by the Norwegian Mapping Authority (NMA).

The objective of making a continuous and regular terrain surface is challenging because both multi-beam and single beam surveys are used in the model. The single beam soundings were sparsely and unevenly distributed, and it was important to use the data to the utmost in order to make a regular grid with 50 m grid space. All the single beam soundings were therefore first used to produce a triangulated irregular network (TIN). From the TIN, a grid with 20 m grid space was generated. The final regular grid modeling with 50 m grid space in UTM WGS84 was based on a compound set consisting of these gridded single beam soundings with original single beam soundings and multi-beam soundings.

5 Model simulations and comparison with measurements

A complete separate set of simulations has been performed for each of the tidal components M_2, S_2, N_2 and K_1 with grid resolution $\Delta x = 100$ m. In order to check the convergence of the solution the M_2 has also been simulated with grid refinement to $\Delta x = 50$ m. Only small negligible differences were detected for flow structures with scale larger then the grid size.

The simulations were started at $t = 0$ with the boundary forcing applied at the open boundaries of the model domain and with a growth factor $(1 - \exp(-\sigma t))$ for a smooth spin-up of the model. A value of $\sigma = 4.6{\cdot}10^{-5}$ s^{-1} has been used which implies full effect of boundary conditions after about 12 hours. At the start the internal fields are all zero ($U = V = \eta = 0$). Steady state oscillations were obtained after a simulation time of 192 hours for the semi-diurnal components and 240 hours for the diurnal component. Entire fields (all grid points) for current and elevation are stored for one tidal period at one hour intervals for each component at the end of the simulations, while for stations within the model area records are kept with three minutes sampling for the whole simulation interval. The time series for the stations have been used to ensure that a steady state oscillation is reached. Harmonic analysis is performed on the full fields and on the time series of the stations yielding amplitude and phase.

Most of the simulations have been made including bottom friction with coefficient $c_D = 0.003$, and runs without friction are performed for comparison. The effect of the boundary conditions applied at the eastern open boundary, east of station 11, fig. 2, has been investigated by including the entire inner Trondheimsfjord in a simulation of

the M_2 component. The area added is roughly of the same size as the main model domain. In this case the two model domains were connected computationally with a Message Passing Interface (MPI) technique . The results of the two simulations shows no significant artificial effect of the open boundary condition.

For comparison with the observations data from three model versions (Mod. I, II and III) are shown in tables 2-3. Mod. I is the regional model with $\Delta x = 500$ m, Mod. II is the standard high resolution model with $\Delta x = 100$ m, and Mod. III is a standard model version with adjustment of the open boundary conditions. The adjustments were primarily designed to improve the fit between observed and modeled phases. For validation of the model we have used data both from sea level and current measurements.

During a period of about 2 months at the end of 2001 and the beginning of 2002 sea level were recorded at five temporary stations Hestvika, Uthaug, Agdenes, Brekstad and Sistranda (fig. 2). In addition data were available from a permanent station Heimsjø. The time series were sampled with 10 minutes interval and harmonic analysis of the data sets were performed (Hareide and Lynge 2002). Harmonic constants based on the available time series from the temporary stations and a 6 year long series from the permanent station are listed in table 2. The data from the station Orkanger, which also is included in the table, are from an earlier and relatively short observation period and the accuracy may be more uncertain.

In the winter and spring 2002 current measurements were made in Trondheimsleia, for the Norwegian oil company Statoil, in two periods each of about 2 months length, along a proposed pipeline route in water depths ranging from 30 to 550 m. Twelve of the recording stations were located within the model domain fig. 2. Most of the measurements were made by sensors located near the sea bed with Aanderaa RCM7 current meters. Acoustic Doppler Current Profilers (ADCP) were used at a few stations to measure the current through the entire water column. We have been given access to this data set which have been reprocessed, checked, and the observed parameters of the current ellipse have been calculated. The results of a comparison with model data for the four major tidal components can be found in a study by Orre et al. (2004).

In this paper we only show the result of the comparison for the largest (M_2) component (tables 2 and 3). The model data are taken from the the model grid point closes to the location of the recording station. For sea level amplitude (tables 2) the three versions of the model are all in good agreement with the observations. There is a slight improved fit for most stations with higher resolution (Mod. II) and boundary value adjustments (Mod. III). The latter model version also shows the best agreement for phases. The observed current data (table 3) are from the first measurement period January-March 2002. The model clearly captures the recorded variation in current speed along the line of stations. A detailed comparison with model data shows good agreement, except for the shallow stations (17 and 18) where the vertical variation in current speed extends through the entire water column.

Additional model simulations with a fully non-linear turbulence closure model has been performed for a subsection of the model domain centered around station 17 and 18 at Proudman Oceanographic Laboratory, UK (J. Xing, private communication, 2003). It is found that the effect of the non-linear advection terms are significant near these stations and that amplitude of the M_4 overtide is about 15 % of M_2 at station 18 and 43 % of M_2 at station 17. From the observational data the corresponding percentages

are calculated to be 14.8 % and 34.5 %. In the main part of the model area the non-linear effects are less important and the depth integrated model (sec. 2) used for this application is therefore a good approximation.

Table 2: Observed and modeled harmonic constants for sea level (M_2)

Stasjon (map code)	*Observed*		*Mod. I*		*Mod. II*		*Mod. III*	
	h *cm*	g *deg*	h *cm*	g *deg*	h *cm*	g *deg*	h *cm*	g *deg*
Heimsjø (Hs)	77.8	301	78.7	298	76.3	296	77.3	301
Hestvika (H)	79.6	304	80.2	300	77.9	298	78.3	302
Uthaug (U)	76.8	303	79.0	301	76.9	300	76.8	303
Agdenes (A)	81.1	304	80.6	299	80.0	298	80.5	303
Brekstad (B)	86.3	306	86.1	301	83.5	299	84.2	304
Sistranda (S)	77.0	303	76.2	299	75.8	299	76.0	302
Orkanger (O)	87.4	306	91.7	300	88.8	298	90.2	303

Table 3: Observed and modeled parameters of current ellipse (M_2). Major and minor half axis A and B, respectively. Orientation of major axis (θ) in degrees true (0 deg. North, 90 deg. East etc.). Rotation of current vector (rot) + clockwise, - anticlockwise). Data for station 7 is depth mean values from ADCP profiles.

Station	Water depth m	Sensor depth m	*Observed*				*Mod. II*			
			A cm/s	B cm/s	θ deg	rot	A cm/s	B cm/s	θ deg	rot
2	220	217	7.61	0.92	71	-	9.87	0.54	69	-
3	115	112	16.46	3.71	90	+	15.72	3.24	85	+
4	275	272	3.00	0.04	43	-	5.83	2.61	66	-
5	360	357	13.32	0.66	50	-	12.68	0.60	59	-
7	410	377	15.10	1.07	152	+	19.31	1.19	152	+
8	520	517	16.00	0.27	26	+	14.26	0.40	10	-
10	550	547	6.55	1.86	161	-	9.85	0.02	166	-
11	500	497	4.65	2.06	71	-	2.38	0.06	73	-
17	80	40	28.23	1.36	99	-	43.15	10.43	113	-
18	50	47	15.71	2.57	108	-	38.74	8.86	165	+

6 Electronic chart systems and the implementation of current fields

There are two basic types of electronic chart systems. Those that comply with the International Maritime Organization (IMO) requirements for SOLAS class vessels (IMO 1986), known as the Electronic Chart Display and Information System (ECDIS), and all other types of electronic charts, regarded generically as, Electronic Chart Systems (ECS).

IMO has developed a performance standard for ECDIS (IMO 1995), which specifies how an ECDIS must work in order to serve as an adequate replacement for paper charts in SOLAS vessels. In order for a type-approved ECDIS to be the legal equivalent of paper charts, the system must display official Electronic Navigational Chart (ENC) data issued by a national Hydrographic Office and complimented by an updating service. The vessel must also have a type-approved back-up system. Official ENCs fulfill the IHO (International Hydrographic Organization) S-57 Standard and have the most recent update from originating National Hydrographic Offices. S-57 (IHO 2000) describes the international standard to be used for exchange of digital hydrographic data between national Hydrographic Offices and for the distribution of digital data and products to manufacturers, mariners and other data users. Another important standard developed by IHO is the S-52 standard (IHO 1996). S-52 provides specifications and guidance regarding the issuing and updating of Electronic Navigational Charts (ENC), and their display in an ECDIS system. S-52 includes color and symbol specifications.

The Norwegian company C-Map has developed the distribution format CM-93/3. This data format is based on the IHO S-57 format and is a more compact format though maintaining the original structure, properties and contents. This compact distribution format has a security mechanism for protecting data from unauthorized modifications and use. The CM-93/3 format is a type approved and S-57 (ed. 3.1) equivalent data format certified by Det norske Veritas (DnV) and can be used as System Electronic Navigational Chart format in the navigation system.

In ECDIS it is possible to include time variable environmental variables like wind, waves and current. These objects are known under the term Marine Information Objects (MIOs). A Harmonization Group on MIO (HGMIO) is established between the International Electro-technical Commission (IEC) and the International Hydrographic Organization (IHO) to deal with MIOs to be used in ECDIS. The primary focus of HGMIO is to developing specifications related to use of MIOs on ECDIS. IHO plans to expand the S-57 and S-52 standards in order to deal with other types of hydrographic data, and a new edition for each standard is planned with target date for completion in 2005 (Alexander, 2003). Specifications for tidal data and tidal current exists in the today edition of both S-57 and S-52

The main objective in this paper has been to develop an example on implementation of tidal current fields in ECDIS. The software "Tidal Current v. 1.1.0" has been developed by the Norwegian company C-MAP Norway A/S for implementation of tidal current in an electronic chart system. As a background in the electronic chart system ENC data on the chart format CM-93/3 has been used. The tidal current vectors are displayed on top of the electronic charts, and appear as a separate layer that can be added or removed from the display.

To get input parameters to the calculation module a graphical dialog window is used. Input data for the calculation module consists of harmonic constants for the four major tidal components M2, S2, N2 and K1 from simulation with model version Mod. I (see sec. 5). For each of the four tidal components, there exist four data files containing the harmonic constants, amplitude and phase in east/west ($\overline{u}$-component) direction and in north/south direction ($\overline{v}$-component) for all oceanic grid points within the model domain.

The tidal current calculation module provides three main functions: Read harmonic constants from the data files, calculate tidal current velocity and direction for a given point and time and provide tidal current information. Following parameters have to be specified before calculating the tidal currents: data source file location, start date, period in days, temporal resolution in minutes and spatial resolution in meters. The tidal currents are calculated from the given parameters and the tidal current vectors are drawn on top of the electronic navigational chart when the calculation is finished. Initially, the first time step is selected and the view is set to an overview of the chosen model area. The user can then zoom and pan to any position and scale, and select date and time in steps of the temporal resolution defined prior to calculation. In the software the tidal current field can also be drawn as a real-time created animation. The calculation time is low, and the application can be used interactively with a low processing delay.

The tidal current vectors are displayed as arrows, indicating direction and velocity of the calculated tidal current at the given position and time. To prevent overlapping in the electronic chart the number of arrows is reduced by a simple algorithm. This algorithm draws either all arrows, every second, every third and so on. In the future this filtering algorithm should be enhanced.

The S-52 specification defines the presentation of tidal current predictions as a dashed three-headed arrow with the velocity in a box on the left side of the arrowhead, and with the time on the right side of the arrow. This means that the user must read the velocity numerically to get an understanding of the strength of the tidal current prediction. As the total number of tidal current vectors is very high in this application, the standard S-52 presentation technique has been replaced by new, simplified symbols that describe the orientation and velocity in a more compact way (see figure 3). The length of a tidal current vector varies from a point representing velocity 0 cm/s and extends to an vector with a maximum length up to 20 cm/s. Current vectors of 20 cm/s and above have a one tail "feather" added for every 20 cm/s. Hence, an arrow describing a tidal current velocity of 40 cm/s will be symbolized as a full-length arrow with two feather tails. The palette follows the S-52 specification, using the color orange for the tidal current vector.

Harmonic constants for new areas can be directly opened by the application as the data files contain coordinates and description of the area. In the future the data format could be converted to a standard XML format to enable other applications to gain access to it.

7 Application examples

The current display system has been implemented in the electronic navigational chart for the entire model domain. Here we show results from two selected areas; The Garten-

Storfosna channel west of Ørlandet near station 17 and 18, and Agdenes at the mouth of the Trondheimsfjord near stations 7 and 8. The examples are from a period with strong tidal currents in late February 2002 due to the coincidence of full Moon and lunar perigee on 27 February.

Fig. 4 shows the current field at the time of peak out-going tide 28 February 2002 at 14 UT displayed on the electronic chart in an overview from the area west of Ørlandet. The next figure (5) shows the current field for the same area 6 hours later at 20 UT nearly at the time of peak in-going tide. The figures 6-8 demonstrate the zooming function of the display with three successive enlargements of the area near station 17 and 18. From fig. 8 the predicted current speed and direction at 14 UT can easily be read from the figure. The current speed is 0.4-0.6 m/s at both stations and the direction is about 330 and 290 degree true at station 17 and 18 respectively. The current speed compare well with the observations, which are 0.56 m/s and 0.58 m/s respectively at the two stations. The observed current direction is 309 and 278 deg. at station 17 and 18 respectively. The deviation between observed and modeled current direction, up to 20 deg., may be due to boundary layer and non-linear advection effects.

Figure 9 is an overview from the area near the mouth of the Trondheimsfjord at the time of peak outgoing tide. The enlargement near the point Agdenes, 3 hours later at the time of low water, shows an eddy structure, with center north of the light (fig. 10). The diameter of the eddy is about 1.5 km. The current speed over the shallow ridge between the light and the headland is up to 1.8 m/s. Unfortunately, there is to our knowledge no current measurements from this area which can confirm this prediction of the model.

8 Concluding remarks

A presentation in a paper does not give a full account of the flexibility of the interactive display of tidal current fields in the electronic chart system. Besides the obvious benefits of the system in providing general information for navigation purposes the system also has the potential for real time display of parameters for special applications. For example the current fields could be used for calculating in real time; drift trajectories for floating objects during rescue operations, forces on vessels during navigation in narrow channels with strong currents, and optimal routing during sailing races etc.

In the demonstration example consider here we may not have used the optimal tidal field, but once the implementation of the system is completed, any updating of the current field can easily be done by changes in the data base for harmonic constants.

The main limitations of the system is of course that the current in a particular location and under certain conditions may deviate considerably from the predicted depth mean tidal current. The deviations can be due to meteorological effects or baroclinic i.e. stratification effects in the water column. The problems with including these effects are that the predictability will be limited to short time spans of a few days and that the current predictions also have to be done at a weather forecasting center onshore with subsequent transfer of the data to the ship.

An alternative way of correcting for the deviations from the calculated depth mean tidal current would be to use observational data from current sensors or buoys in the area. This method could be feasible for narrow limited area or channels where the ship traffic is monitored. Corrected and updated current fields could then be used directly

by the traffic controllers or transmitted to ships and displayed on the electronic chart system onboard.

With a simple ship based system as demonstrated here only the predictable barotropic tidal current and the associated sea level changes can be displayed. In many situations information of this part of the total current field may be important for a correct assessment of the environmental conditions influencing the maneuverability and the safety of ships or marine operations.

Acknowledgment
The modeling work has been supported by The Norwegian Research Council under a grant from the BeMatA programme. We are grateful to Statoil, Norway, by its representative Mr. Einar Nygaard for being given access to current data from the measurement programme in Trondheimsleia. The participation by Mr. Noralf Slotsvik, NHS in the planing of this project is greatly appreciated.

References

[1] Aksland, K.O. 2002. Manual for processing bathymetric data. Norwegian Hydrographic Service, Stavanger, Norway. 15 pp. (In Norwegian)

[2] Alexander, L. 2003. Marine Information Objects (MIOs) and ECDIS: Concept and Practice. U.S. Hydrographic Conference, 24-27 March 2003, Biloxi, MS, USA.

[3] CM-93 Edition 3.0. C-MAP Norway AS. 2pp.

[4] CMN 2003. Global Electronic Chart Service. C-MAP Norway AS.

[5] Davies, A. M., Jones, J. E., and Xing, J. 1997a. Review of recent development in tidal hydrodynamic modeling. I: Spectral Models. J. Hydraulic Engineering. Vol. 123, NO. 4, p. 278-292.

[6] Davies, A. M., Jones, J. E., and Xing, J. 1997b. Review of recent development in tidal hydrodynamic modeling. II: Turbulence Energy Models. J. Hydraulic Engineering. Vol. 123, NO. 4, p. 293-302.

[7] Foreman, M. G. G. 1978. Manual for Tidal Current Analysis and Prediction. Pacific Marine Science Report 78-6. Institute of Ocean Sciences, Patricia Bay, Sidney. British Columbia.

[8] Gjevik, B. 1990. Simulations of shelf sea response due to traveling storms. Preprint Series 2/90. Dept. Math. University of Oslo, Norway.

[9] Gjevik, B., Nøst, E., and Straume, T. 1994. Model simulations of the tides in the Barents Sea. J. Geophys. Res., Vol 99, No C2, 3337–3350.

[10] Hareide, D. and Lynge, Kjoss, B. 2001. Water level observations from Trondheimsleia and Frohavet. December 2001-February 2002. Report GEO 02-2, Norwegian Hydrographic Service, Stavanger, Norway. 18pp.

[11] IHO. 2003. What are a Electronic Chart Systems.
URL: "http://www.iho.shom.fr/ECDIS/introduction.htm".

[12] NHS. 2002. Electronic Chart Systems - a brief introduction. Norwegian Hydrographic Service, Stavanger, Norway. 3pp.

[13] International Convention for the Safety of Life at Sea (SOLAS). International Maritime Organization.

[14] IEC. 2000. Maritime navigation and radio communication equipment and systems - electronic chart display and information system (ECDIS) - operational and performance requirements, methods of testing and required test results. International Electrotechnical Commission. 85pp.

[15] IHO. 1997. IHO S-52. Specification for Chart Content and Display Aspects of ECDIS. International Hydrographic Organization.

[16] IHO. 1998. IHO Standards for Hydrographic Surveys, International Hydrographic Organization, Special Publication No 44, 4th Edition. 23 pp.

[17] Kongsberg Simrad. 1999. Neptune. Post-processing system for bathymetric data. Product description. Kongsberg Maritime, Horten, Norway. 26 pp.

[18] Martinsen, E. A., and Engedahl, H. 1987. Implementation and testing of a lateral boundary scheme as an open boundary condition in a barotropic ocean model. Coastal Engineering. Vol. 11, p. 603-627.

[19] Martinsen, E. A., Gjevik, B., and Røed, L. P. 1979. A numerical model for long barotropic waves and storm surges along the western coast of Norway. J. Phys. Oceanography Vol.9, No 6, 1126-1138.

[20] Mesinger, F., and Arakawa, A. 1976. Numerical methods used in atmospheric models. Garp Publication Series No 17, WMO-ICSU.

[21] Moe, H., Gjevik, B., and Ommundsen, A. 2003. A high resolution tidal model for the coast of Møre and Trøndelag, western Norway. Norwegian Journal of Geography. Vol. 57, 65-82.

[22] Ofstad, A.E., and Haustveit, K-T. 2000. Error estimates using multi-beam echo sounder in hydrographic surveying. Report GEO 00-2, Norwegian Hydrographic Service, Stavanger, Norway. 21 pp. (In Norwegian)

[23] Orre, S., Åkervik, E. and Gjevik, B. 2004. Analysis of current and sea level observations from Trondheimsleia. Preprint Series, No. 1. Dept. Math. University of Oslo, Norway (ISSN 0809-4403).

[24] Schwiderski, E. W. 1980. On charting global ocean tides. Rev. Geophysics. Vol. 18, p. 243-268.

[25] Øvstedal, S. 2002. Prosesshåndbok Forsert sjømåling. Hydrographic Surveying Manual. Norwegian Hydrographic Service, Stavanger, Norway. 22 pp. (In Norwegian)

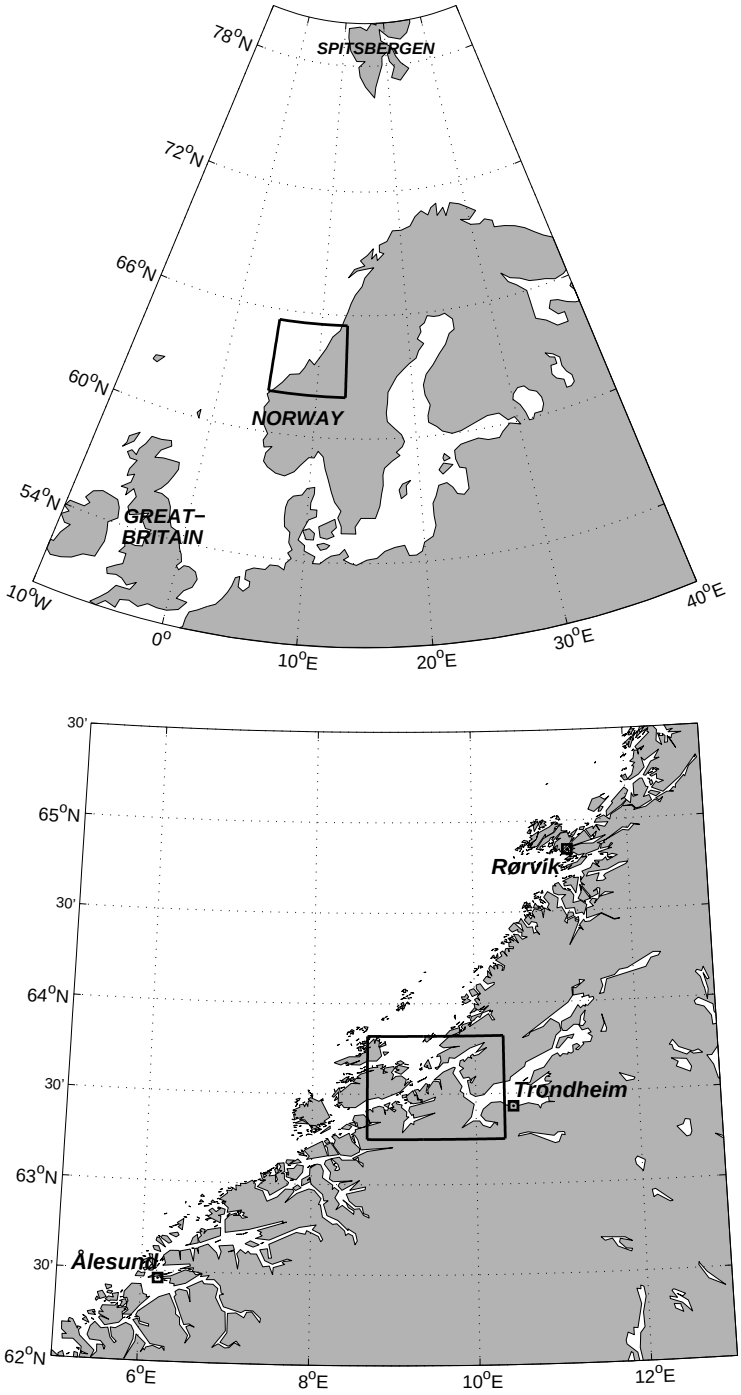

Figure 1: Location of the model domains on the western coast of Norway. The regional model domain is marked with a square box on the upper map. Lower map shows a blow up of the regional model domain with the high resolution model domain in Trondheimsleia marked with a rectangle.

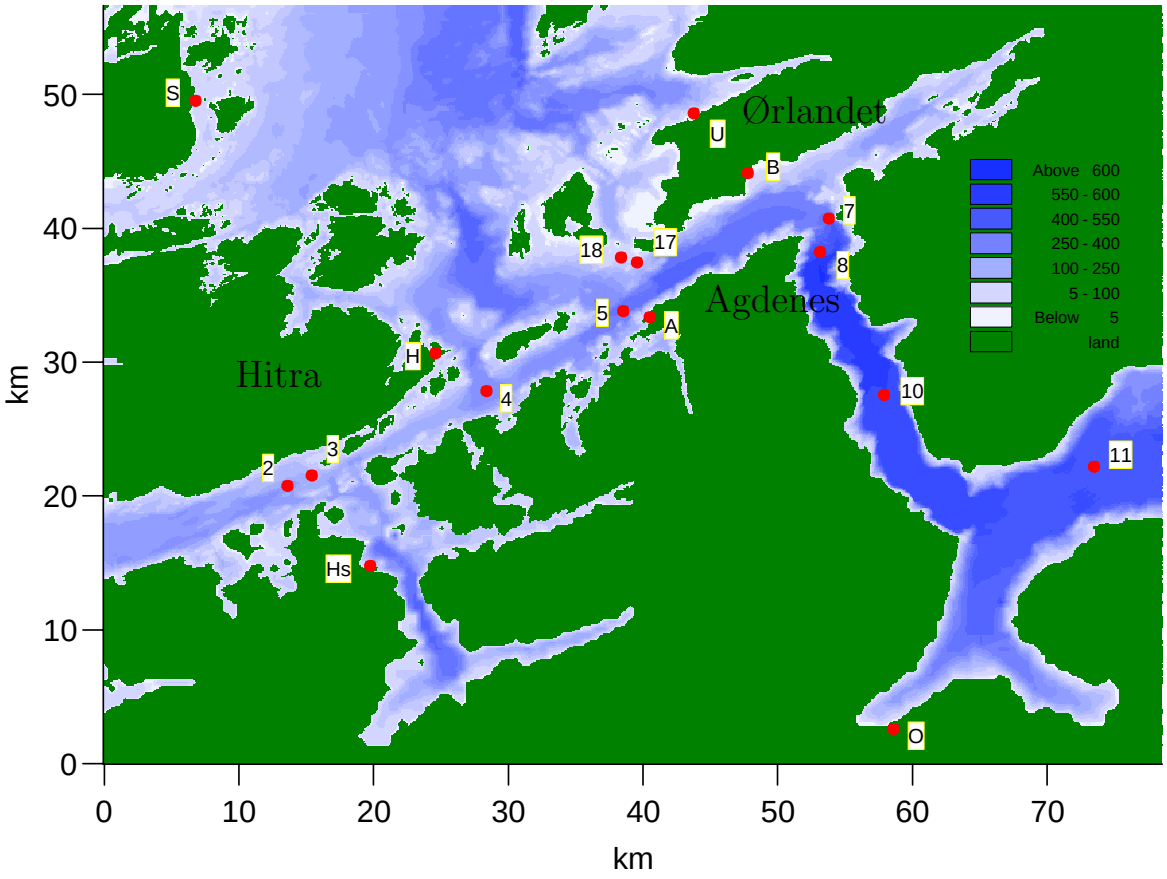

Figure 2: Model domain in Trondheimsleia and stations with current and sea level measurements. The location of the domain is marked on the regional map in fig. 1. Depth (meter) in color scale.

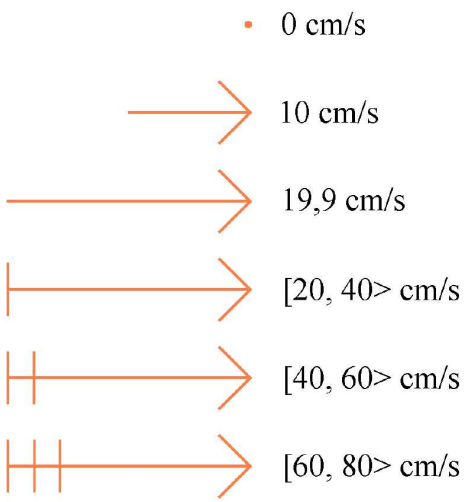

Figure 3: Scaling of current vectors

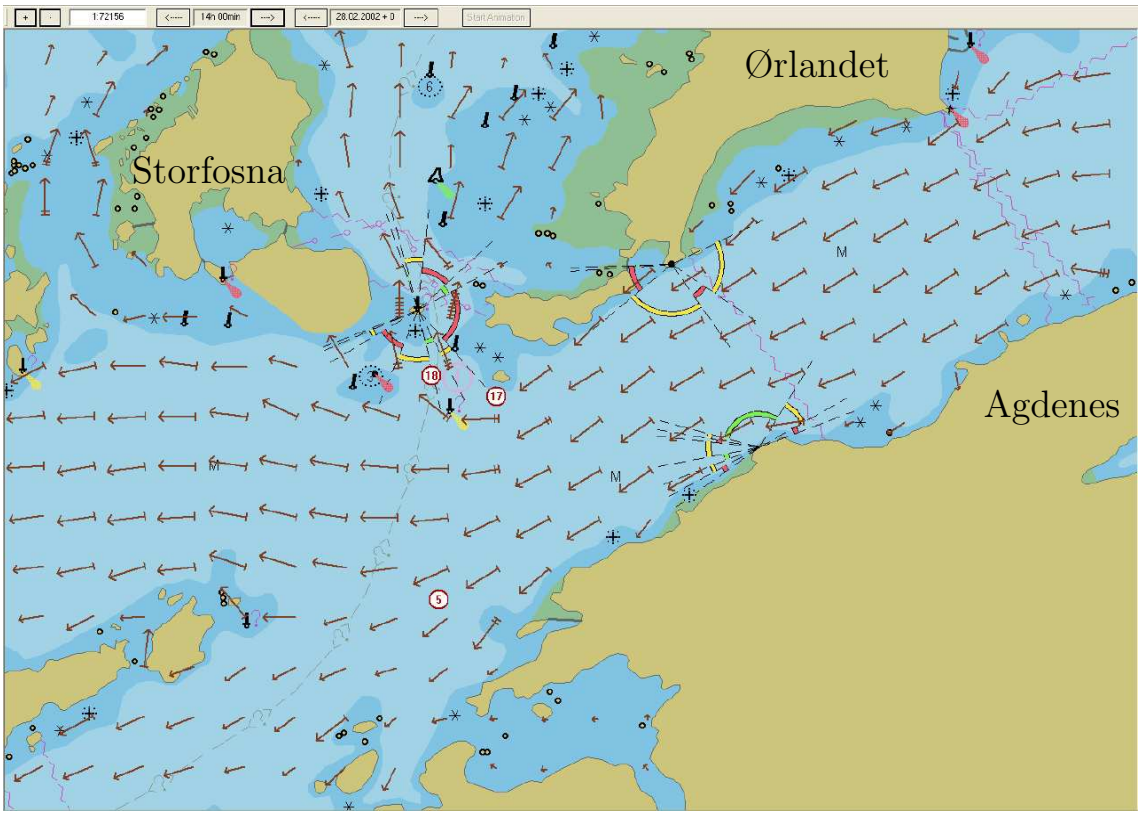

Figure 4: The screen display of the electronic navigational chart for a section of Trondheimsleia southwest of Ørlandet at the time of the peak out-going (ebb) tidal current. 28 February 2002, 14:00 UT. Position of recording stations 5, 17, and 18 marked.

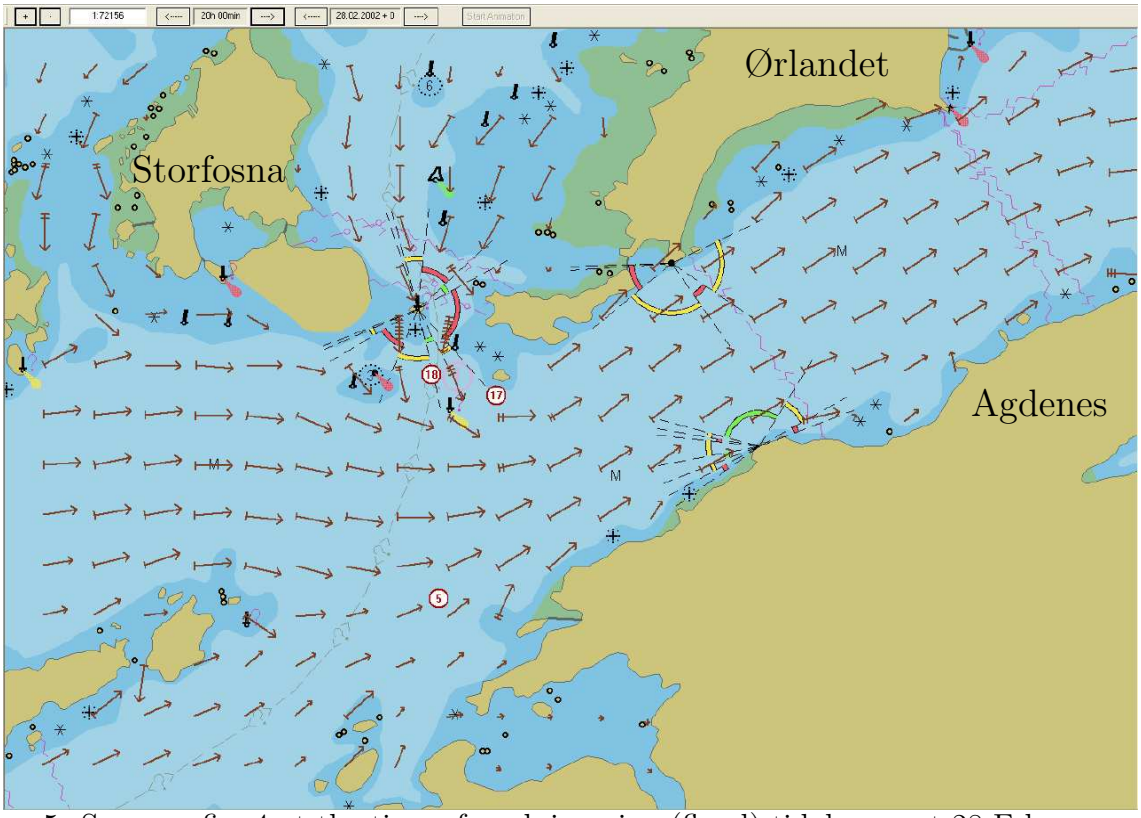

Figure 5: Same as fig. 4 at the time of peak in-going (flood) tidal current 28 February 2002 20:00 UT.

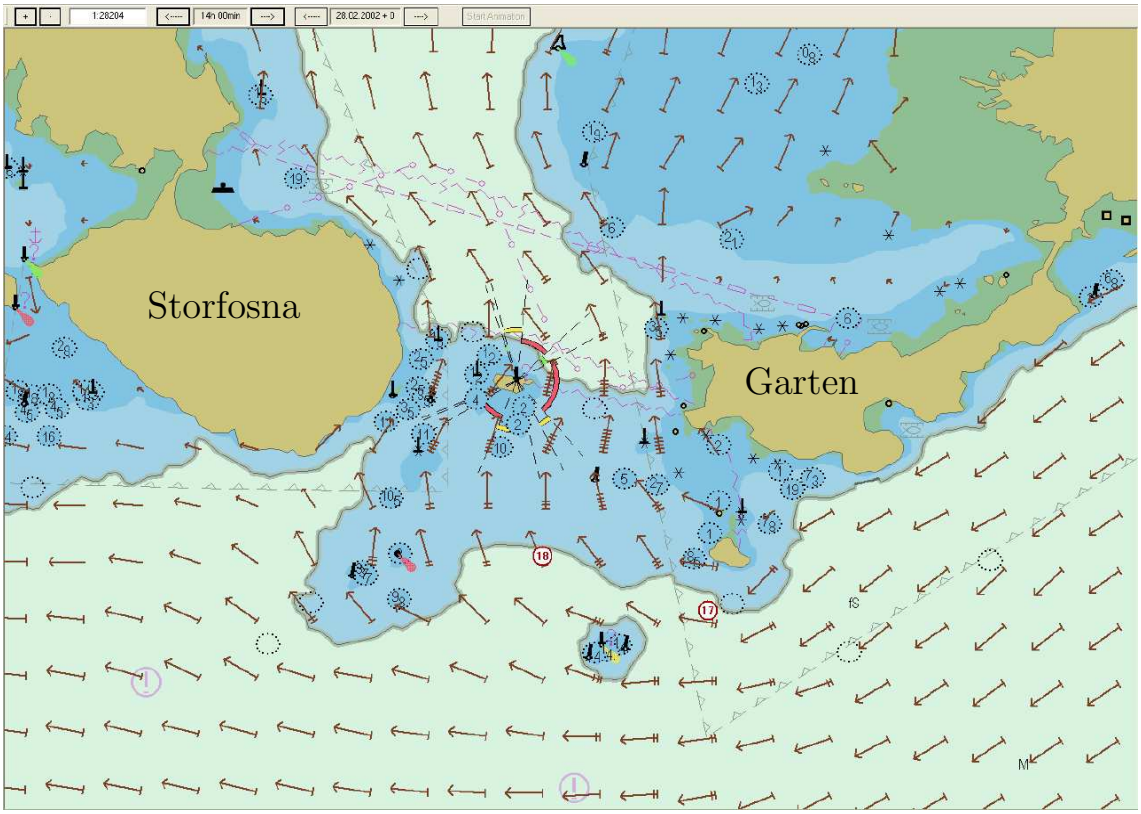

Figure 6: Zoom 1; 28 February 2002 14:00 UT.

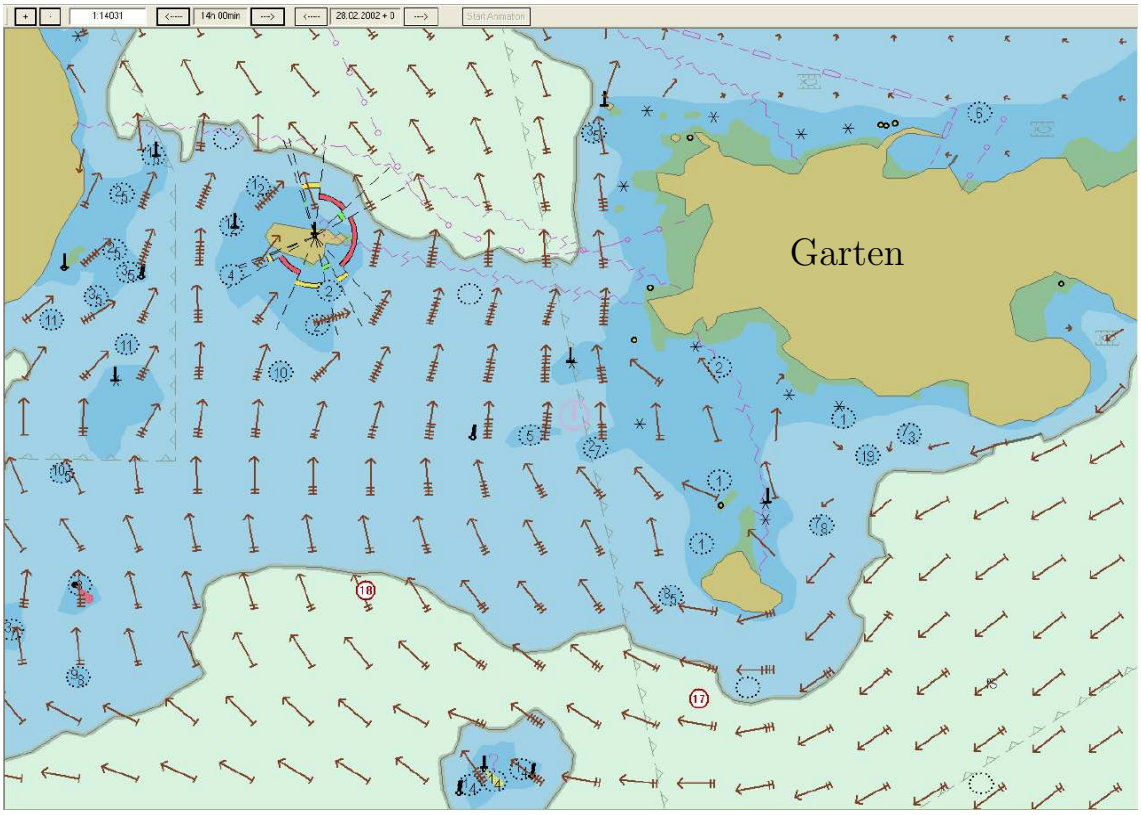

Figure 7: Zoom 2; 28 February 2002 14:00 UT.

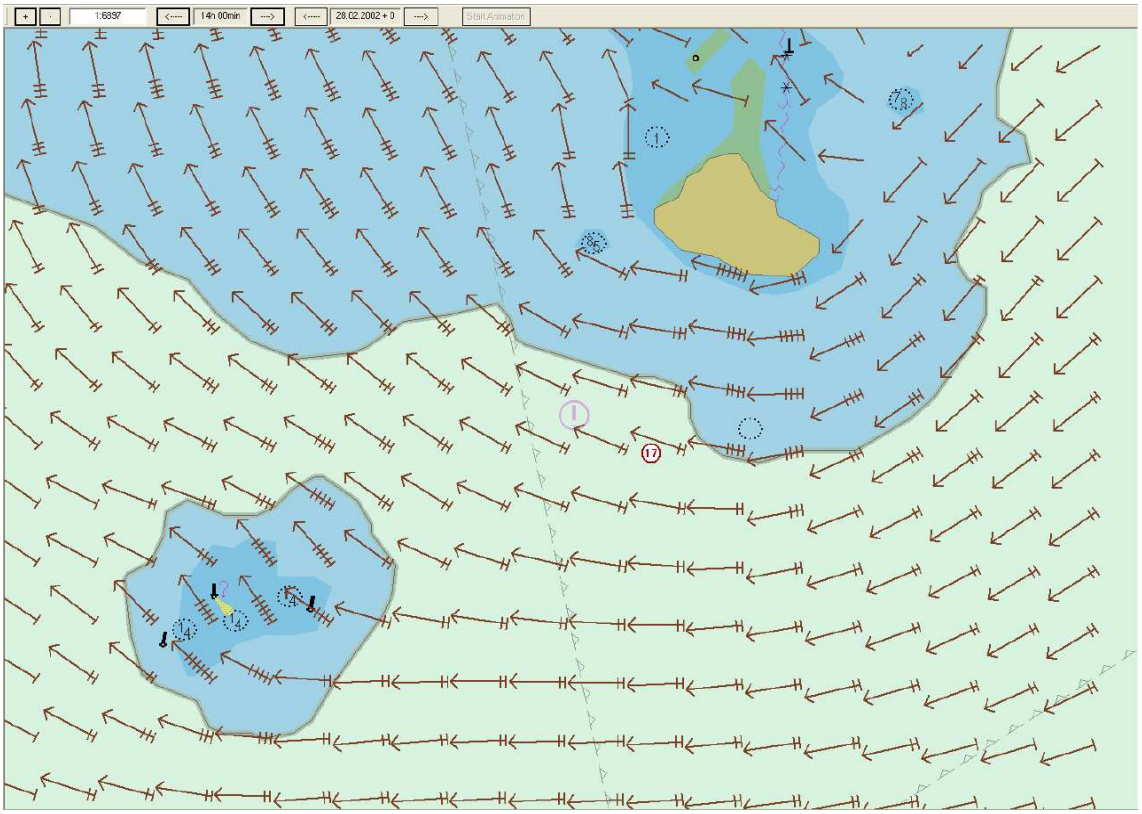

Figure 8: Zoom 3; 28 February 2002 14:00 UT.

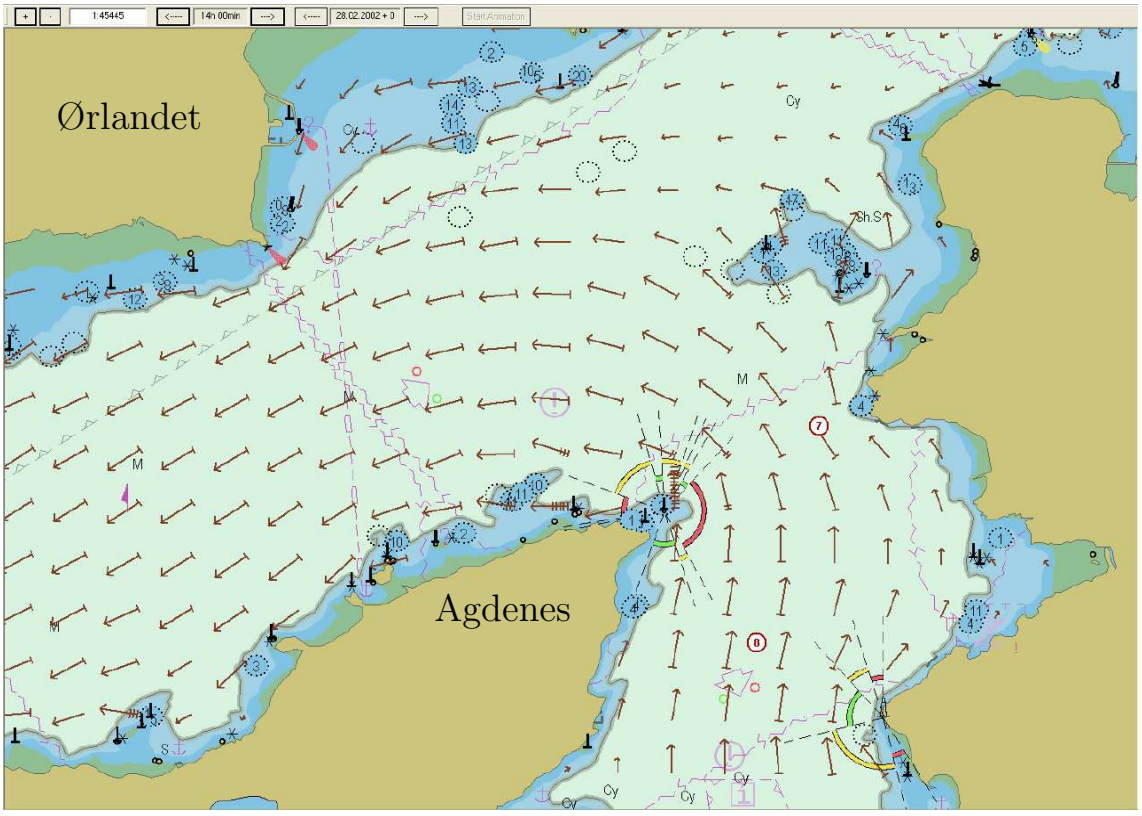

Figure 9: The screen display of the electronic navigational chart near Agdenes at the time of the peak out-going (ebb) tidal current. 28 February 2002, 14:00 UT. Position of recording stations 7, and 8 marked.

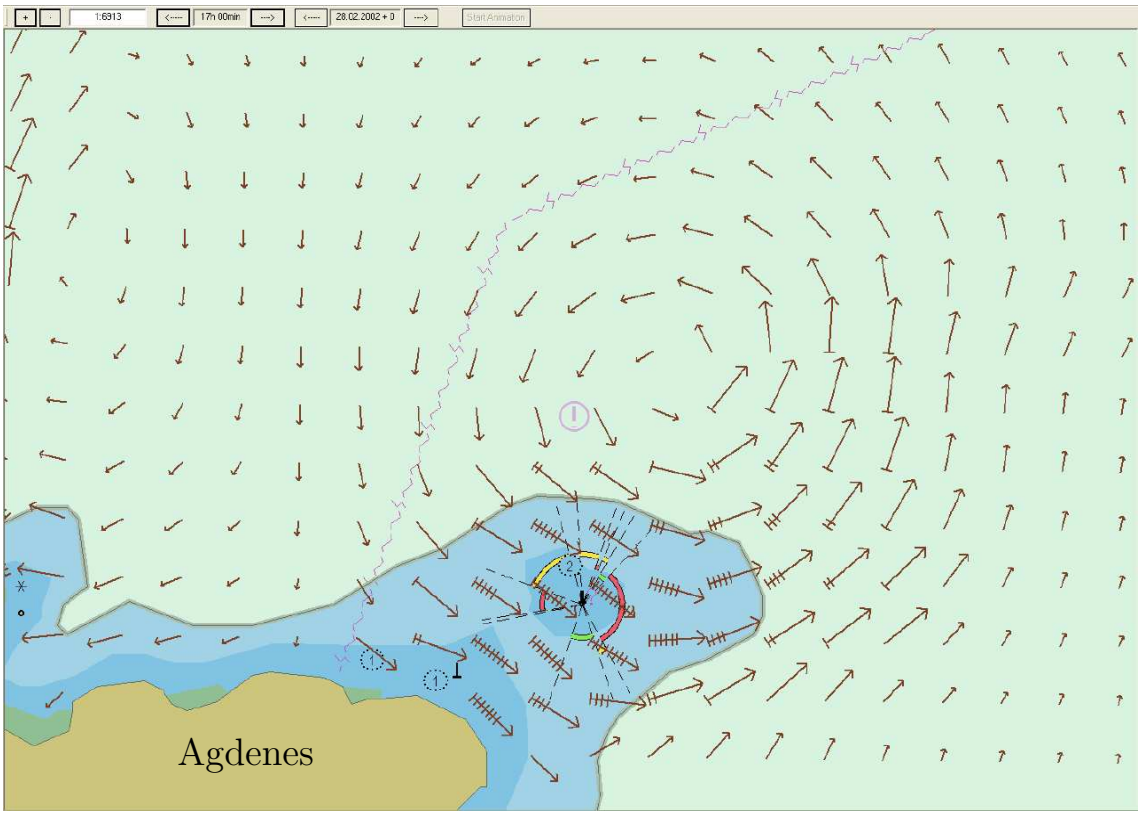

Figure 10: Zoom Agdenes; 28 February 2002 17:00 UT.